

# ADJOINT METHODS IN A HIGHER- ORDER SPACE-TIME DISCONTINUOUS-GALERKIN SOLVER FOR TURBULENT FLOWS

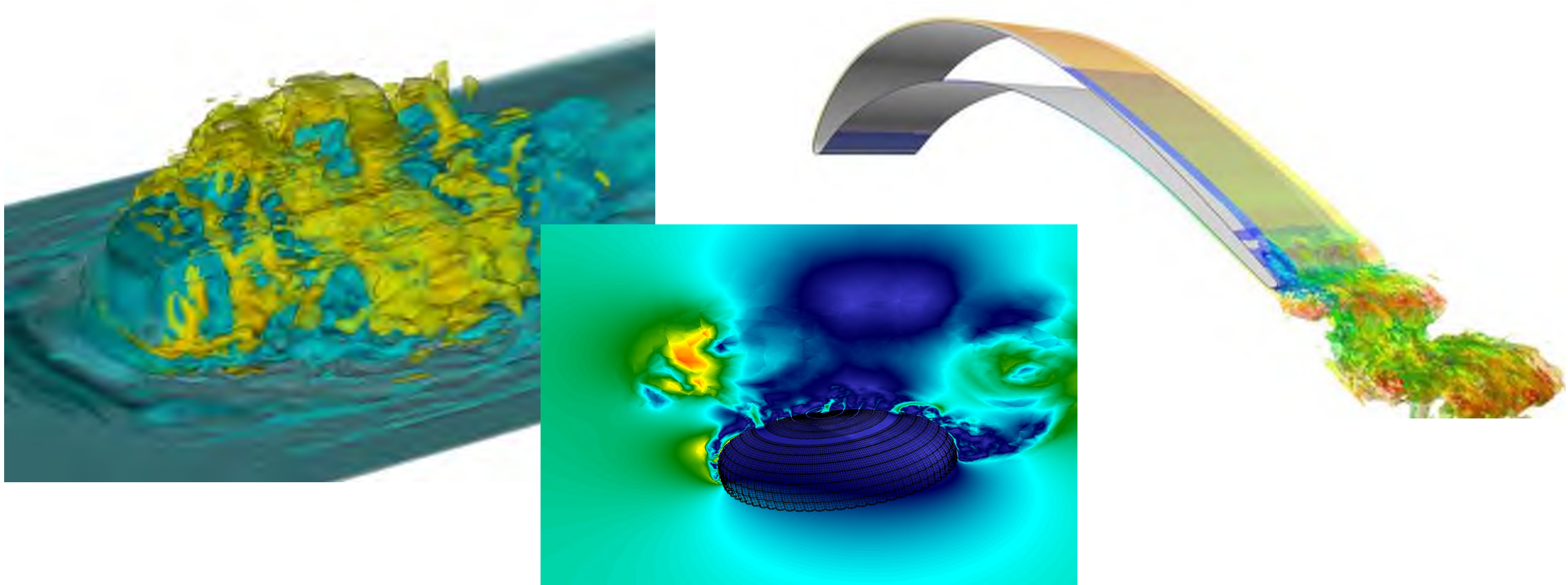
Laslo Diosady  
Science & Technology Corp.

Patrick Blonigan  
USRA

Scott Murman  
NASA ARC

Anirban Garai  
Science & Technology Corp.

# Motivation



- Perform detailed time-accurate scale-resolving simulations of practical, complex, compressible flows
- High-Reynolds-number separated flows involving large-scale unsteadiness, where RANS models are unreliable



# Approach

- Turbulent flows involve a large range of spatial and temporal scales which need to be resolved
- Efficient algorithms and implementation necessary for wall-resolved high Reynolds number flows
- Numerical method must be capable of handling complex geometry
- Numerical method must be “robust”

**Developed higher-order space-time discontinuous-Galerkin spectral element framework**



# Approach

- Gradient computation needed for error-estimation, adaptation, design, sensitivity analysis, etc.
- Tangent and adjoint methods have been successfully applied to a variety of steady and unsteady flows
- High-fidelity simulations we are targeting are chaotic
- Can traditional tangent/adjoint methods work?
- **Develop efficient implementation of tangent and adjoint method in space-time discontinuous solver**
- **Assess the applicability of traditional adjoint and tangent methods for chaotic flows**





# Outline

- Space-time DG formulation
  - Discrete primal formulation
  - Discrete tangent and adjoint formulations
- NACA0012
  - Flow sensitivity with increasing Reynolds number
  - Properties of adjoint for chaotic flows
- T106a LPT
  - Adjoint solutions corresponding to a practical simulation
- Summary/Outlook



# Space-Time Discontinuous-Galerkin (DG) Formulation

- Compressible Navier-Stokes Equations:  $\frac{\partial u}{\partial t} + \nabla \cdot F(u, \nabla u) = 0$

- Space-Time Discontinuous-Galerkin Discretization:

- Entropy variables: Hughes (1986)

$$\begin{array}{ccc} \text{SPD} & \text{Sym} & \text{SPSD} \\ \downarrow & \downarrow & \downarrow \\ A_o v_{,t} + A_i v_{,i} - (K_{ij} v_{,j})_{,i} = 0 \end{array}$$

$$v = \begin{bmatrix} -\frac{s}{\gamma-1} + \frac{\gamma+1}{\gamma-1} - \frac{\rho E}{p} \\ \frac{\rho u_i}{p} \\ -\frac{\rho}{p} \end{bmatrix}$$

- Inviscid Flux: Ismail & Roe (2009)
- Viscous Flux: Interior penalty method with penalty parameter given by 2nd method of Bassi and Rebay (2007)
- Integrals evaluated using numerical quadrature with 2N points
- Discrete entropy stability: Barth (1995)

$$(\rho s)_{,t} + \left( \frac{q_i}{c_v T} \right)_{,i} = v_{,i}^T K_{ij} v_{,j} \geq 0$$

# Discrete Formulation

- Discrete system solved each time-slab:

$$R^n(u^n, w^n) + G^n(u^{n-1}, w^n) = 0$$

- where:

$$R^n(u^n, w^n) = \sum_{\kappa} \left\{ \int_I \int_{\kappa} - \left( \frac{\partial w}{\partial t} u + \nabla w \cdot F \right) + \int_I \int_{\partial \kappa} w \widehat{F \cdot n} + \int_{\kappa} w(t_-^{n+1}) u(t_-^{n+1}) \right\}$$

$$G^n(u^{n-1}, w^n) = \sum_{\kappa} \left\{ \int_{\kappa} -w(t_+^n) u(t_-^n) \right\}$$

- beginning/end of time-slab

$$w(t_+^n) = I_s w^n \qquad w(t_-^{n+1}) = I_e w^n$$

# Discrete Tangent formulation

- Output:  $J(u; \alpha)$ 
  - where  $\alpha$  is a parameter (i.e. angle of attack, Reynolds number etc.)
- Compute sensitivity of output to parameters:

$$\frac{dJ}{d\alpha} = \frac{\partial J}{\partial \alpha} + \frac{\partial J}{\partial u} \frac{\partial u}{\partial \alpha} = \frac{\partial J}{\partial \alpha} + \frac{\partial J}{\partial \bar{R}} \frac{\partial \bar{R}}{\partial \alpha}$$

- Tangent equation:

$$\frac{\partial R^n}{\partial u^n} (\delta u^n, w^n) + \frac{\partial G^n}{\partial u^{n-1}} (\delta u^{n-1}, w^n) = - \frac{\partial R^n}{\partial \alpha}$$

- Matrix form:

$$\begin{bmatrix} \frac{\partial R^{n-1}}{\partial u^{n-1}} & 0 & 0 \\ \frac{\partial G^n}{\partial u^{n-1}} & \frac{\partial R^n}{\partial u^n} & 0 \\ 0 & \frac{\partial G^{n+1}}{\partial u^n} & \frac{\partial R^{n+1}}{\partial u^{n+1}} \end{bmatrix} \begin{bmatrix} \delta u^{n-1} \\ \delta u^n \\ \delta u^{n+1} \end{bmatrix} = - \begin{bmatrix} \frac{\partial R^{n-1}}{\partial \alpha} \\ \frac{\partial R^n}{\partial \alpha} \\ \frac{\partial R^{n+1}}{\partial \alpha} \end{bmatrix}$$



# Discrete Adjoint Formulation

- Lagrangian:  $\mathcal{L}(u, \psi; \alpha) = J(u; \alpha) + \psi^T \bar{R}(u; \alpha)$

- Stationarity of Lagrangian:

$$\delta \mathcal{L} = \underbrace{\left( \frac{\partial J^T}{\partial u} \bigg|_{\alpha} + \psi^T \frac{\partial \bar{R}}{\partial u} \bigg|_{\alpha} \right)}_{\text{Adjoint}} \delta u + \underbrace{\left( \frac{\partial J^T}{\partial \alpha} \bigg|_u + \psi^T \frac{\partial \bar{R}}{\partial \alpha} \bigg|_u \right)}_{\text{Sensitivity}} \delta \alpha = 0$$

- Adjoint equation:

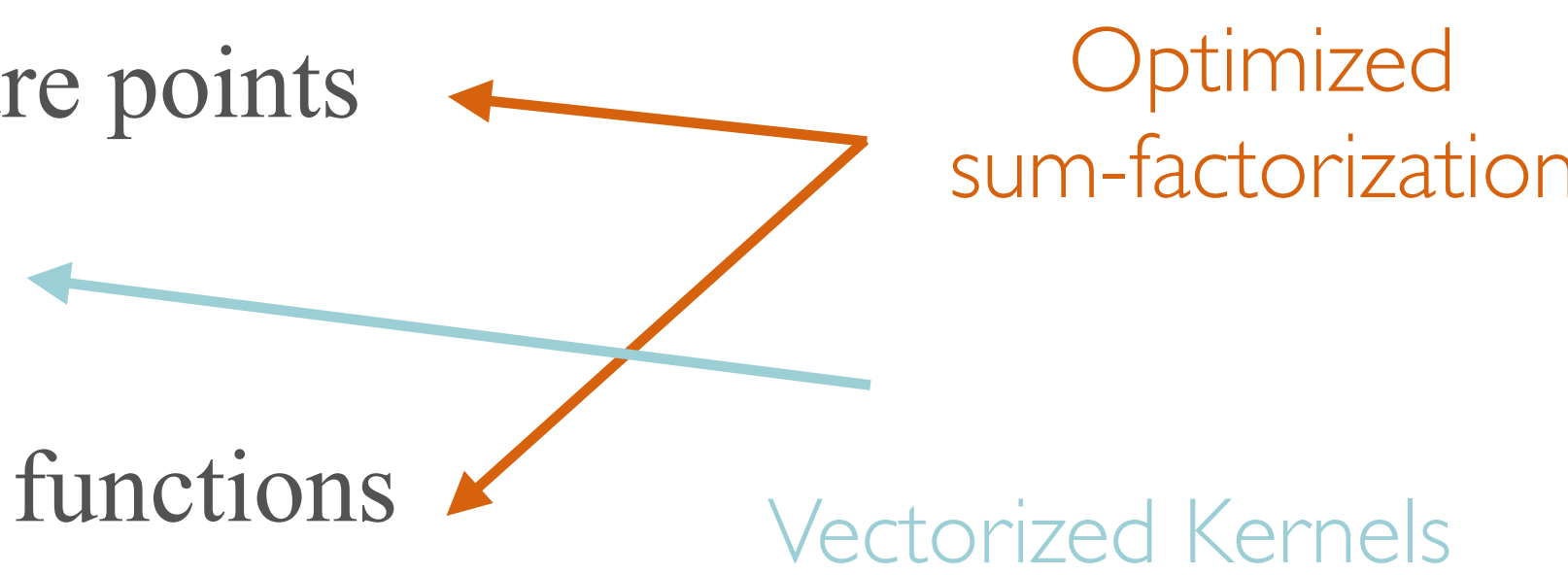
$$\frac{\partial R^n}{\partial u^n}(w^n, \psi^n) + \frac{\partial G^n}{\partial u^{n-1}}(w^{n-1}, \psi^n) = -\frac{\partial J^n}{\partial u^n}(\psi^n)$$

- Matrix Form:

$$\begin{bmatrix} \frac{\partial R^{n-1}}{\partial u^{n-1}}^T & \frac{\partial G^n}{\partial u^{n-1}}^T & 0 \\ 0 & \frac{\partial R^n}{\partial u^n}^T & \frac{\partial G^{n+1}}{\partial u^n}^T \\ 0 & 0 & \frac{\partial R^{n+1}}{\partial u^{n+1}}^T \end{bmatrix} \begin{bmatrix} \psi^{n-1} \\ \psi^n \\ \psi^{n+1} \end{bmatrix} = - \begin{bmatrix} \frac{\partial J^{n-1}}{\partial u^{n-1}} \\ \frac{\partial J^n}{\partial u^n} \\ \frac{\partial J^{n+1}}{\partial u^{n+1}} \end{bmatrix}$$

# Primal Solver: Implementation Details

- **Efficient implementation of higher order DG**
  - Tensor-product basis
  - Take advantage of hardware (SIMD/optimized kernels)
  - Jacobian-free Approximate Newton-Krylov solver
  - Tensor-product based ADI-preconditioner
- **Primal Residual Evaluation:**

1. Evaluate state/gradient at quadrature points
  2. Evaluate flux at quadrature points
  3. Weight fluxes with gradient of test functions
- 
- Optimized sum-factorization
- Vectorized Kernels

# Tangent/Adjoint: Implementation Details

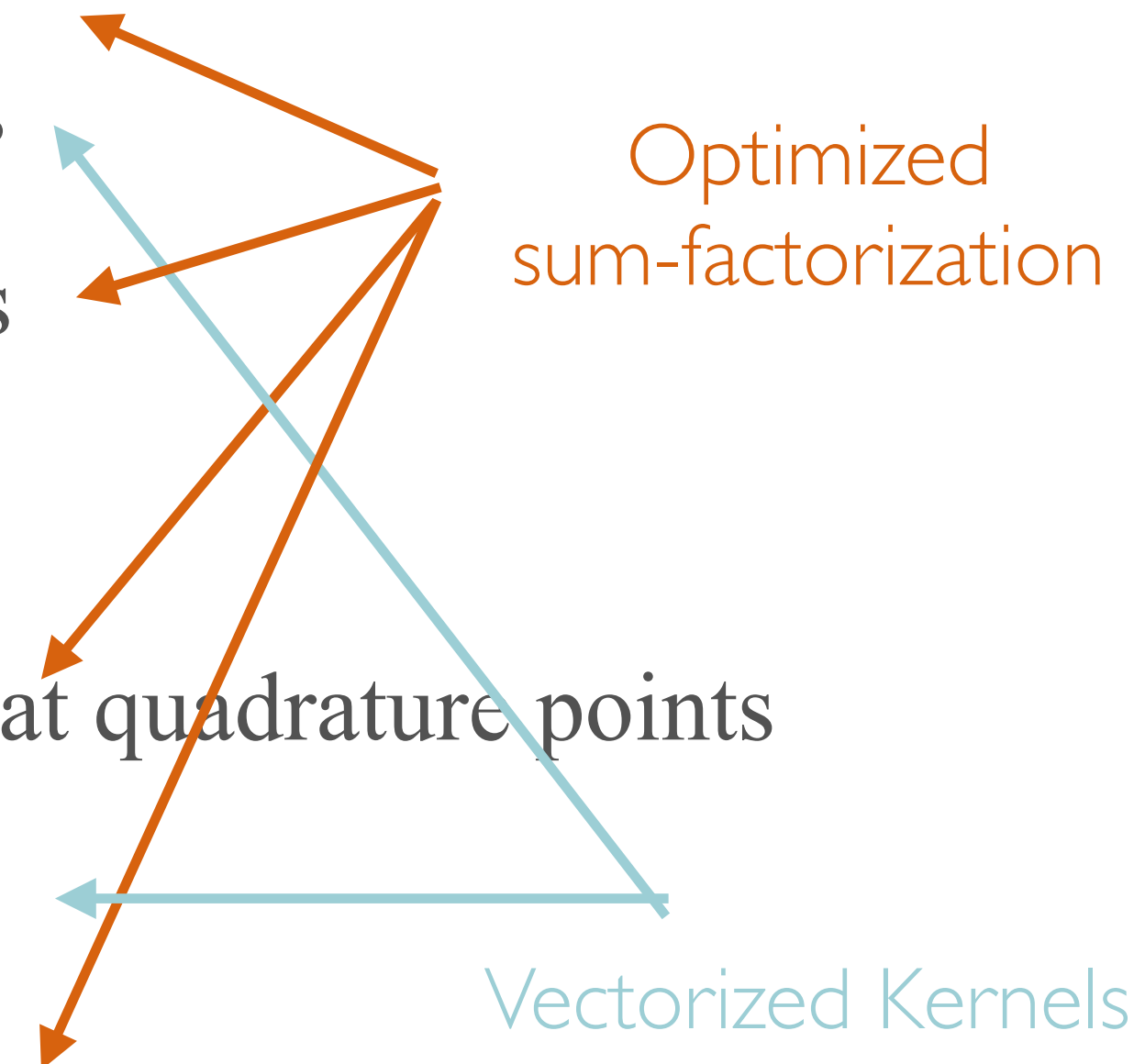
- **Reuse optimization from primal for tangent and adjoint**

- Tangent Residual Evaluation:

1. Evaluate state/gradient and update/gradient at quadrature points
2. Evaluate linearized flux at quadrature points
3. Weight fluxes with gradient of test functions

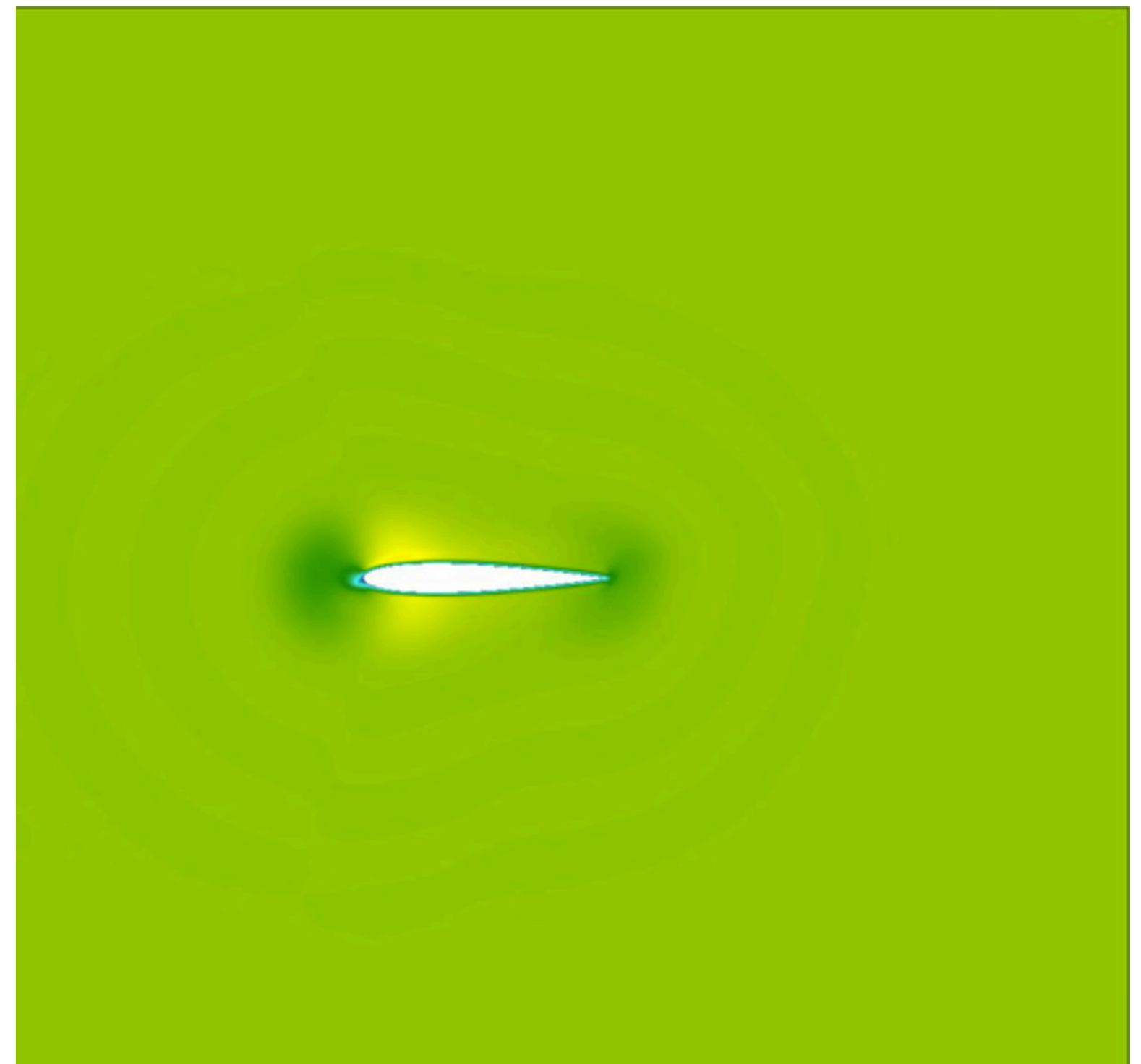
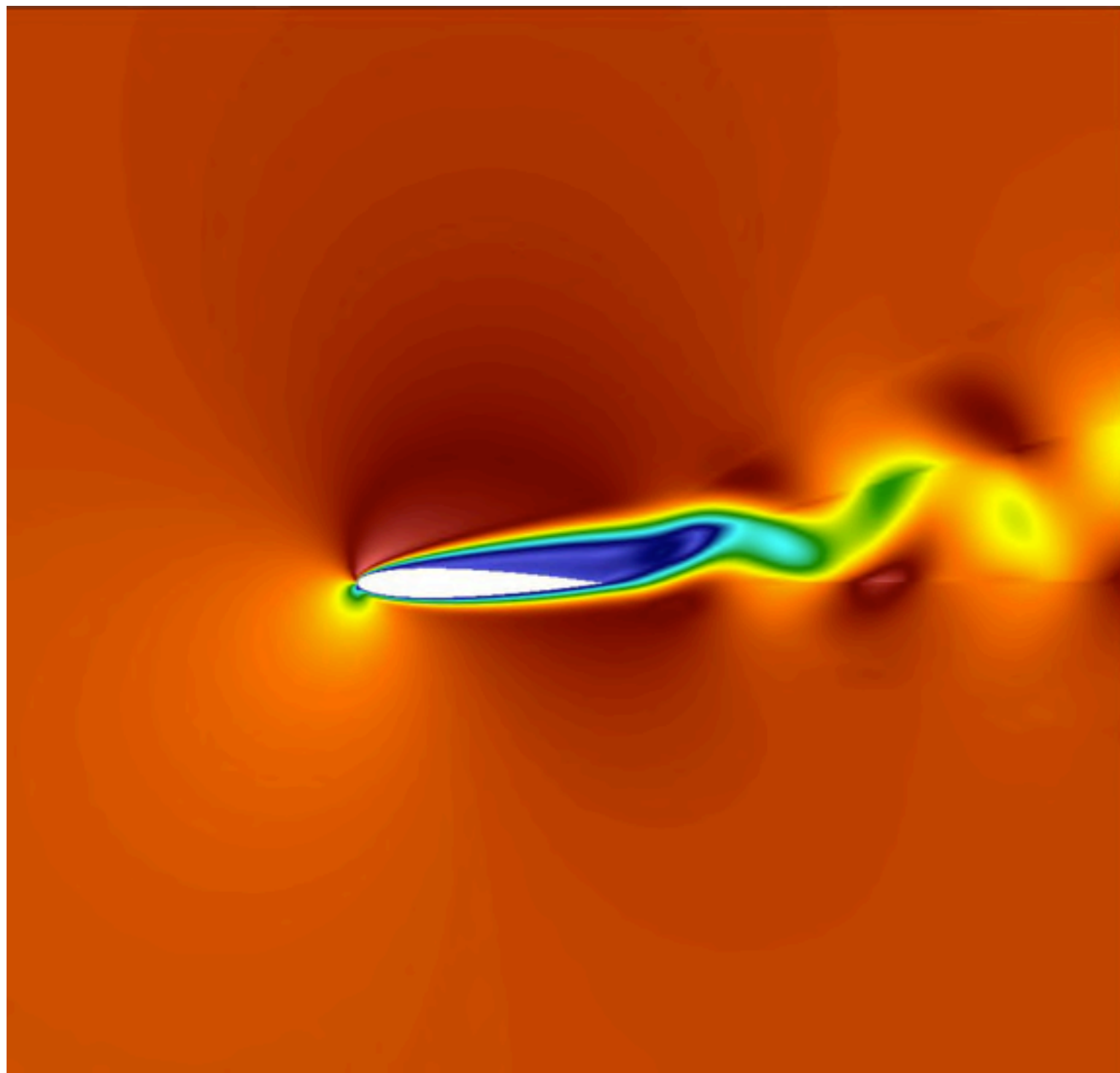
- Adjoint Residual Evaluation:

4. Evaluate state/gradient and adjoint/gradient at quadrature points
5. Evaluate adjoint flux at quadrature points
6. Weight fluxes with gradient of test functions

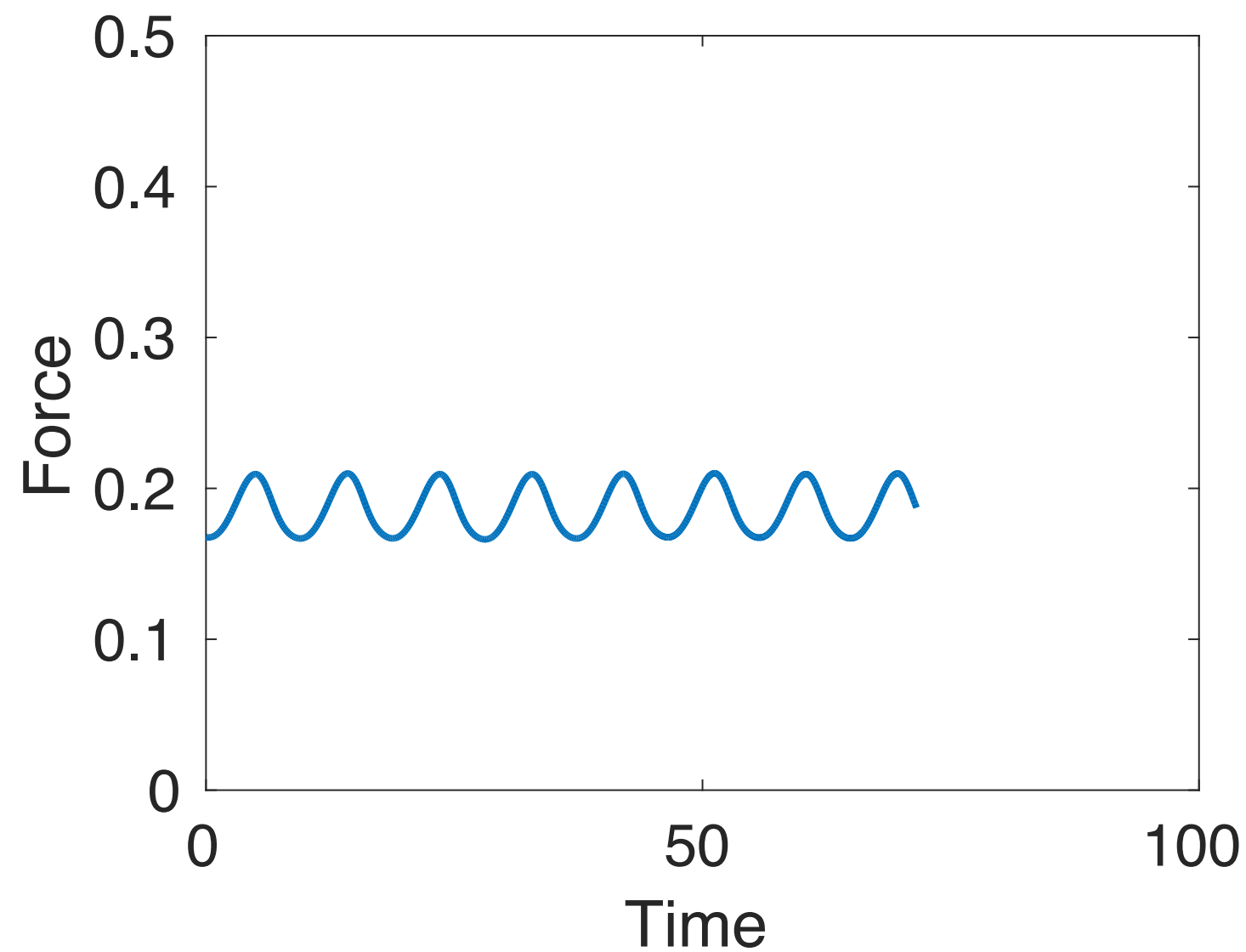


# NACA0012, $\alpha = 10$

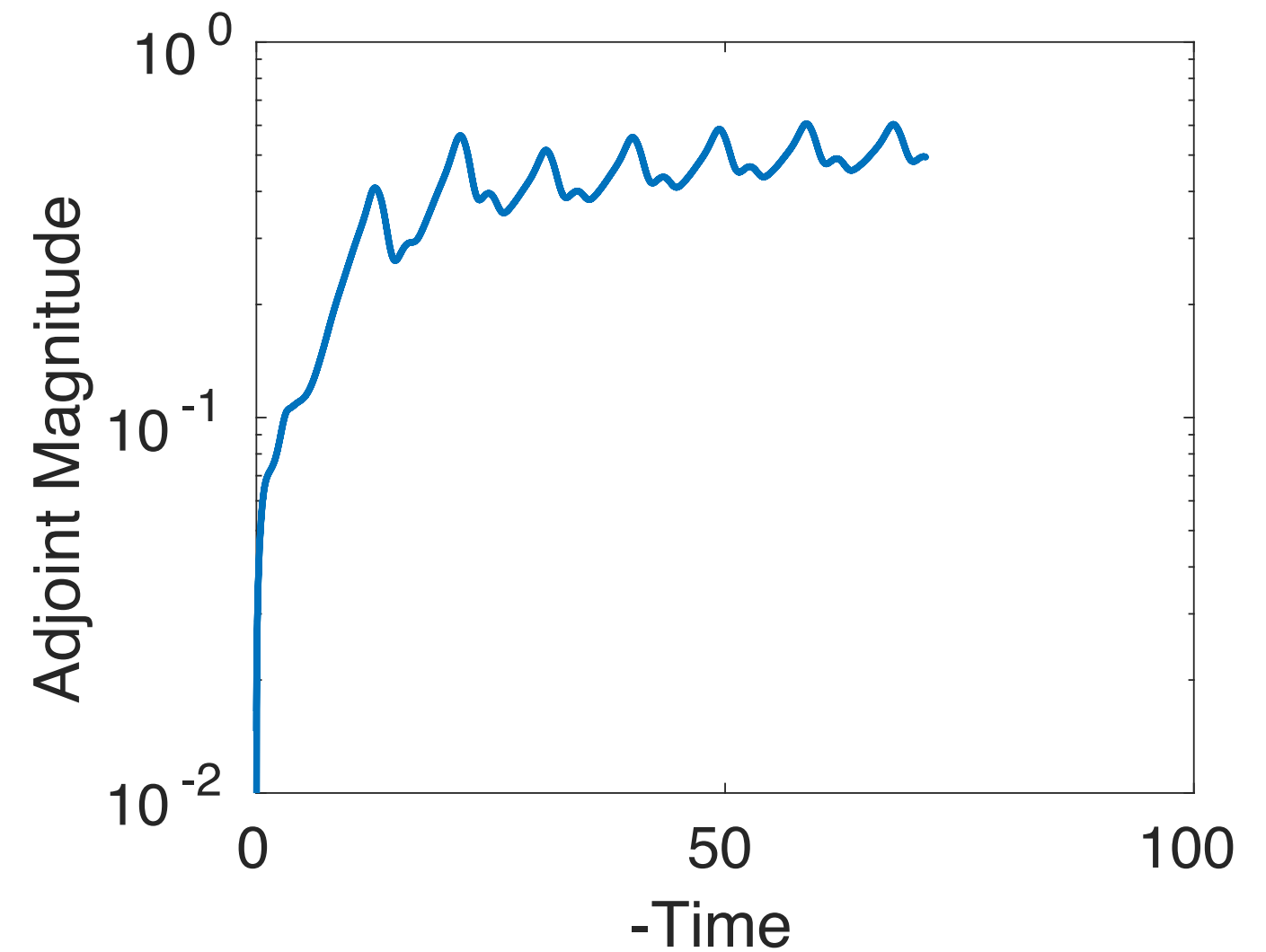
- At high angle of attack, flow over NACA0012 airfoil exhibits vortex shedding which become chaotic with increasing Reynolds number. (Pulliam 1993)
- Examine primal and adjoint solutions



# NACA0012, $Re = 800$ , $\alpha = 10$



Directional Force Output

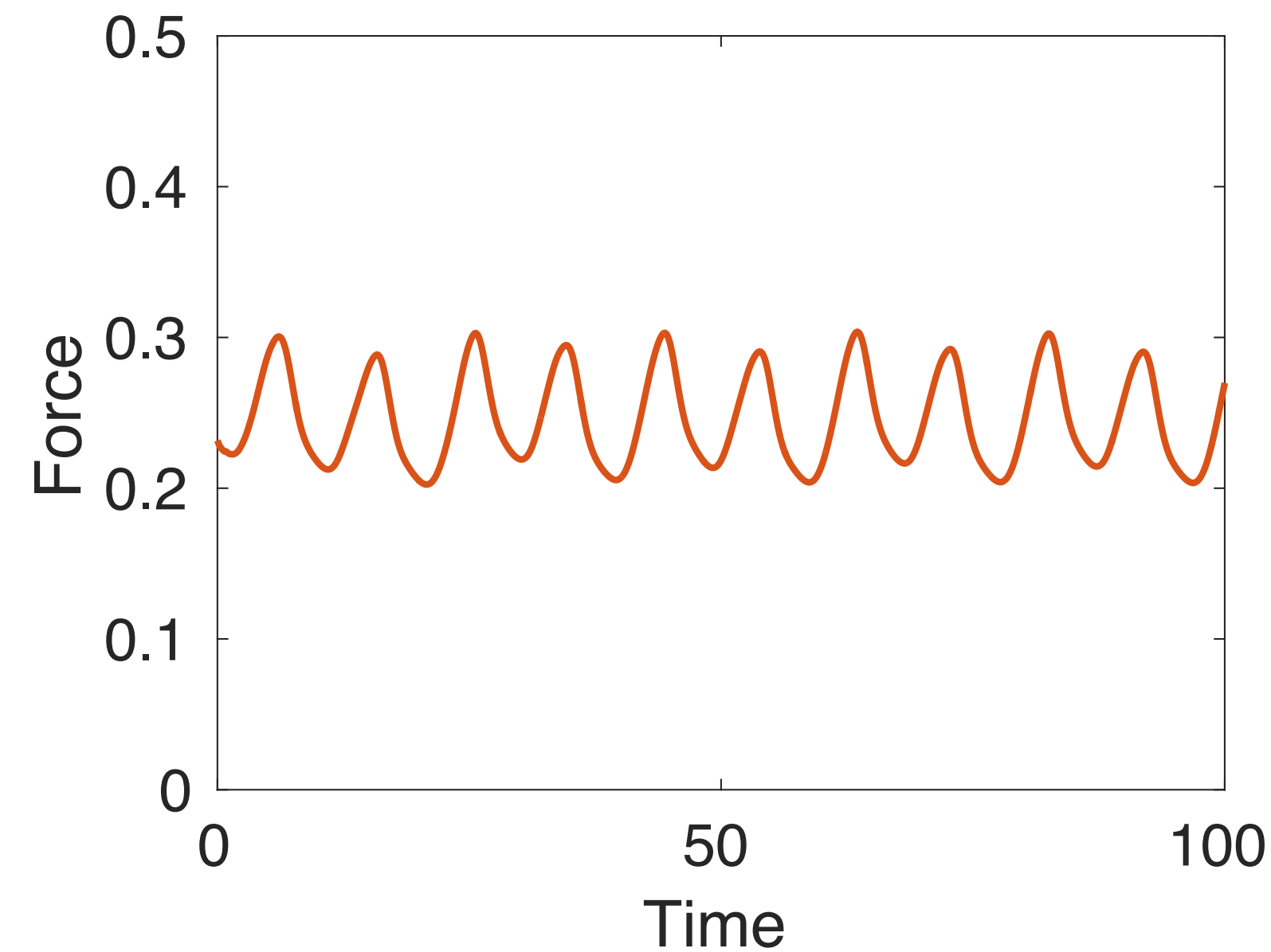


Adjoint Magnitude

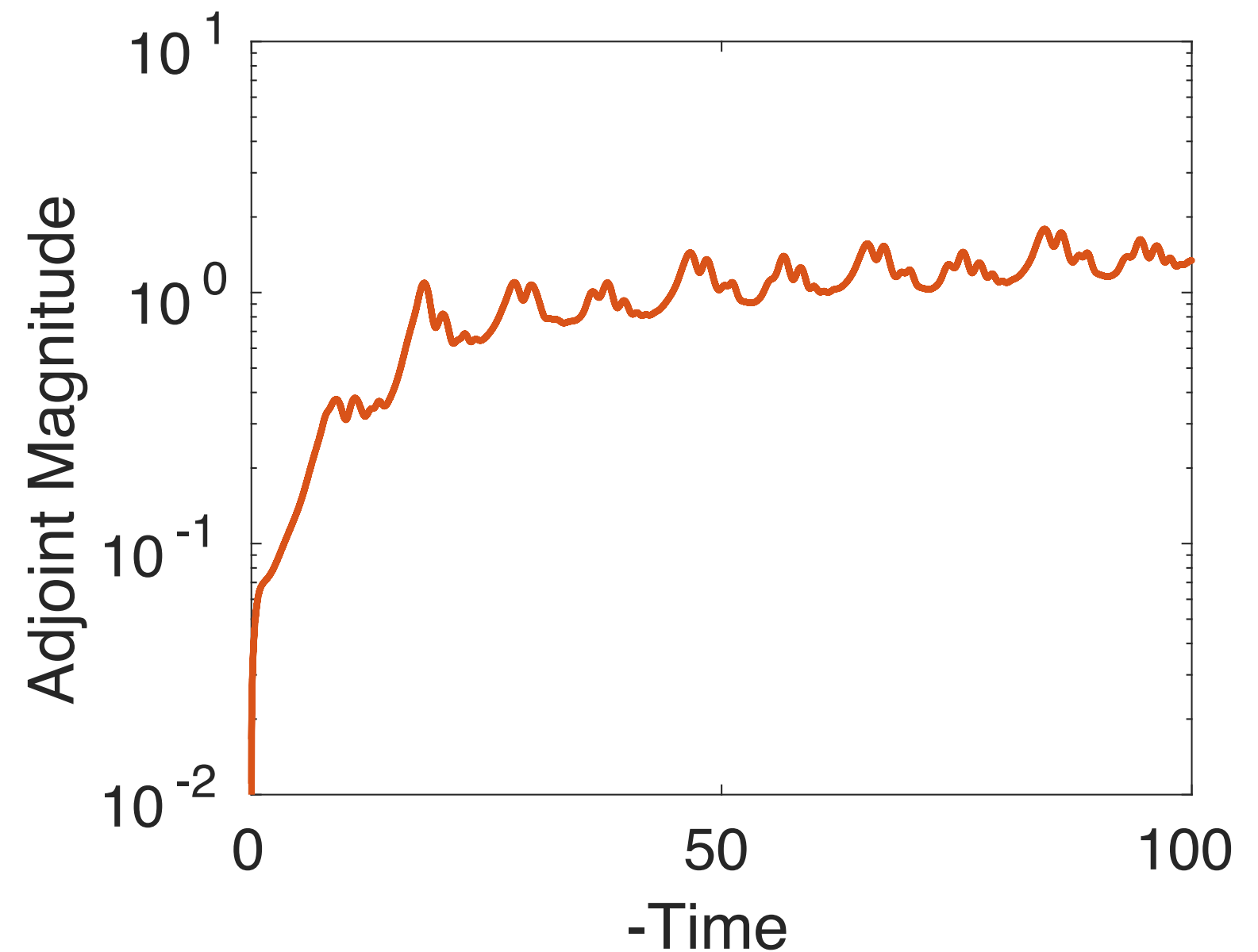
- Unsteady shedding gives periodic output signal
- Adjoint solution also periodic (after initial transient)



# NACA0012, $Re = 1600$ , $\alpha = 10$



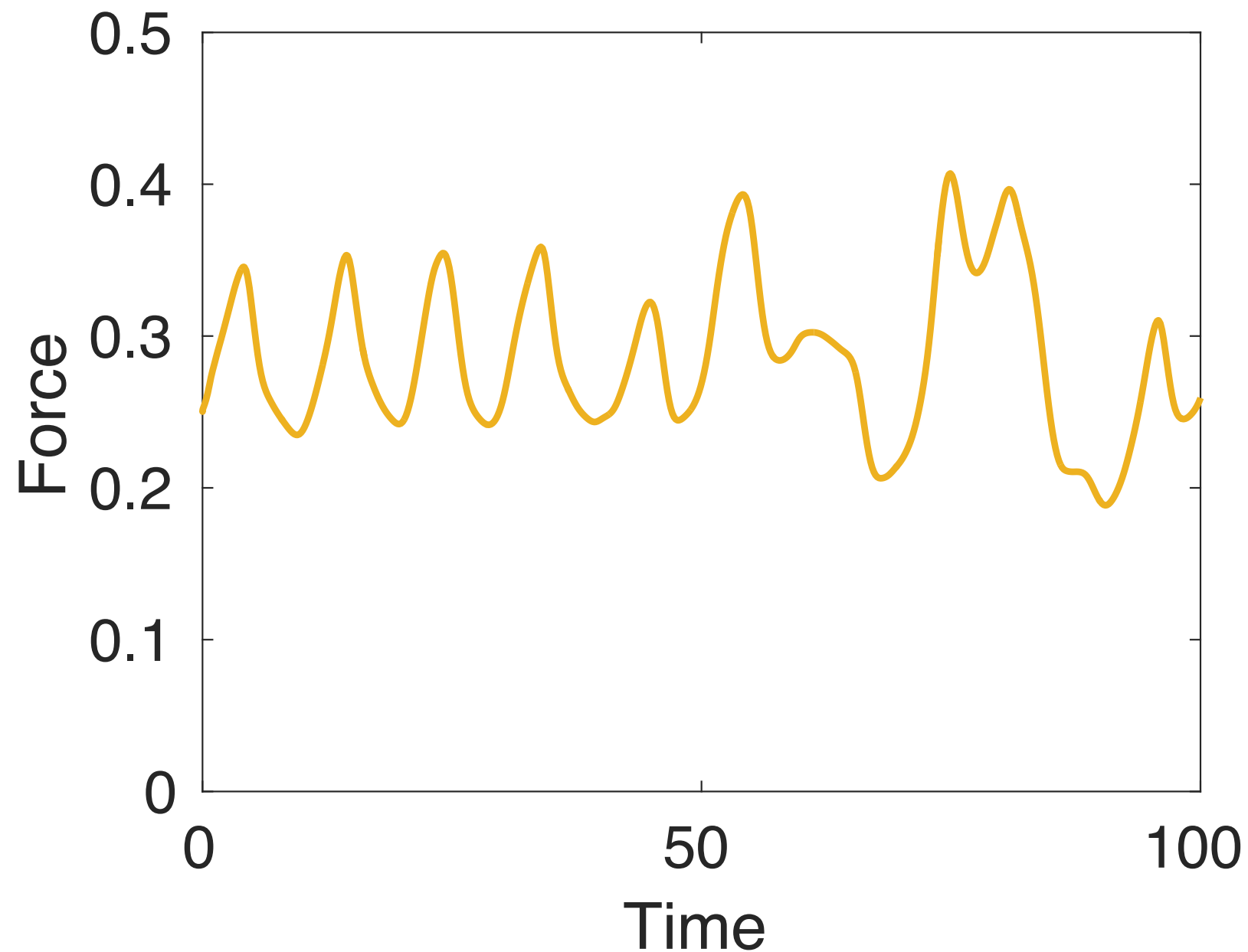
Directional Force Output



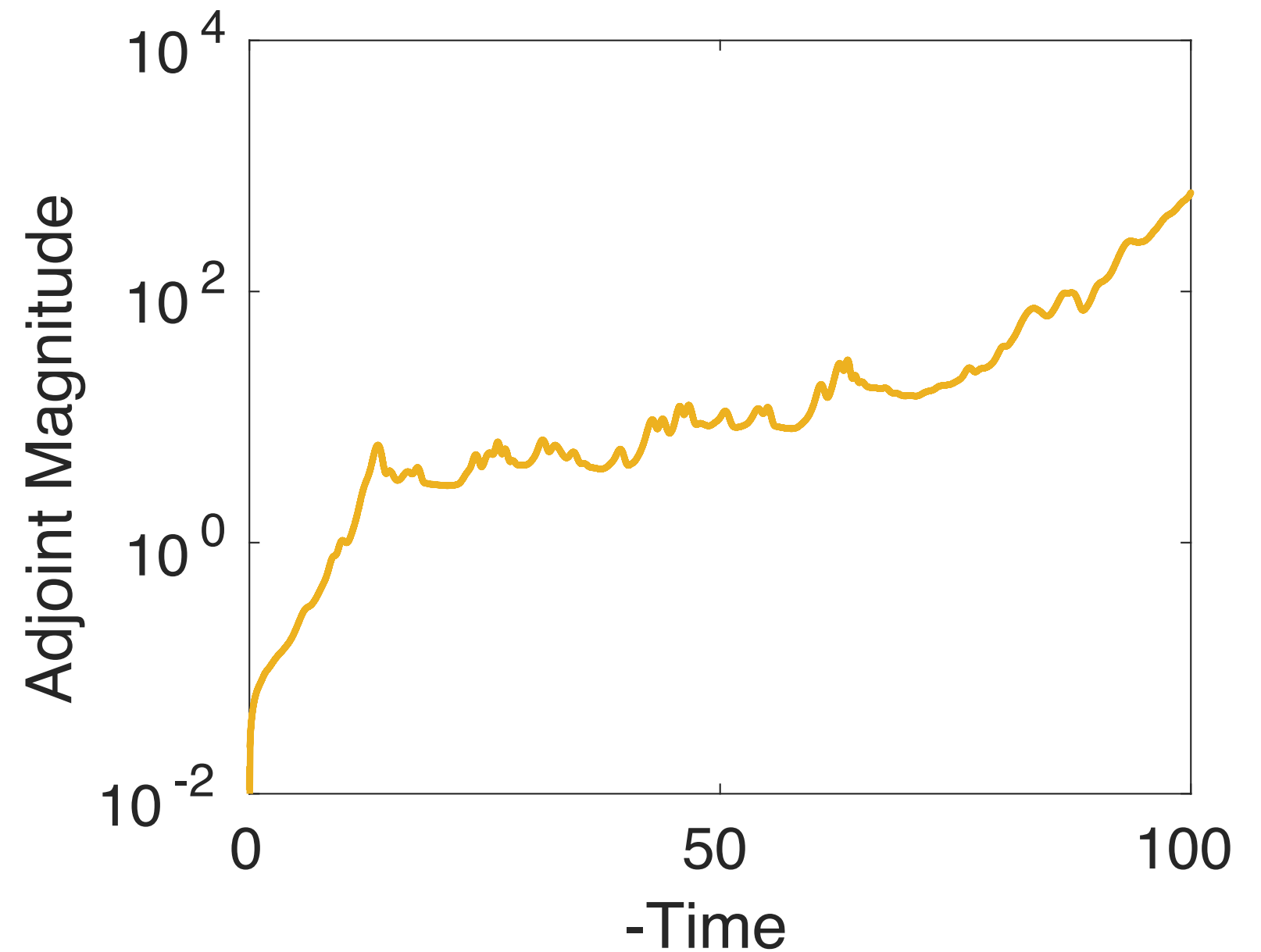
Adjoint Magnitude

- With increasing Reynolds number force has multiple frequencies
- Adjoint solution still essentially appears periodic

# NACA0012, $Re = 2400$ , $\alpha = 10$



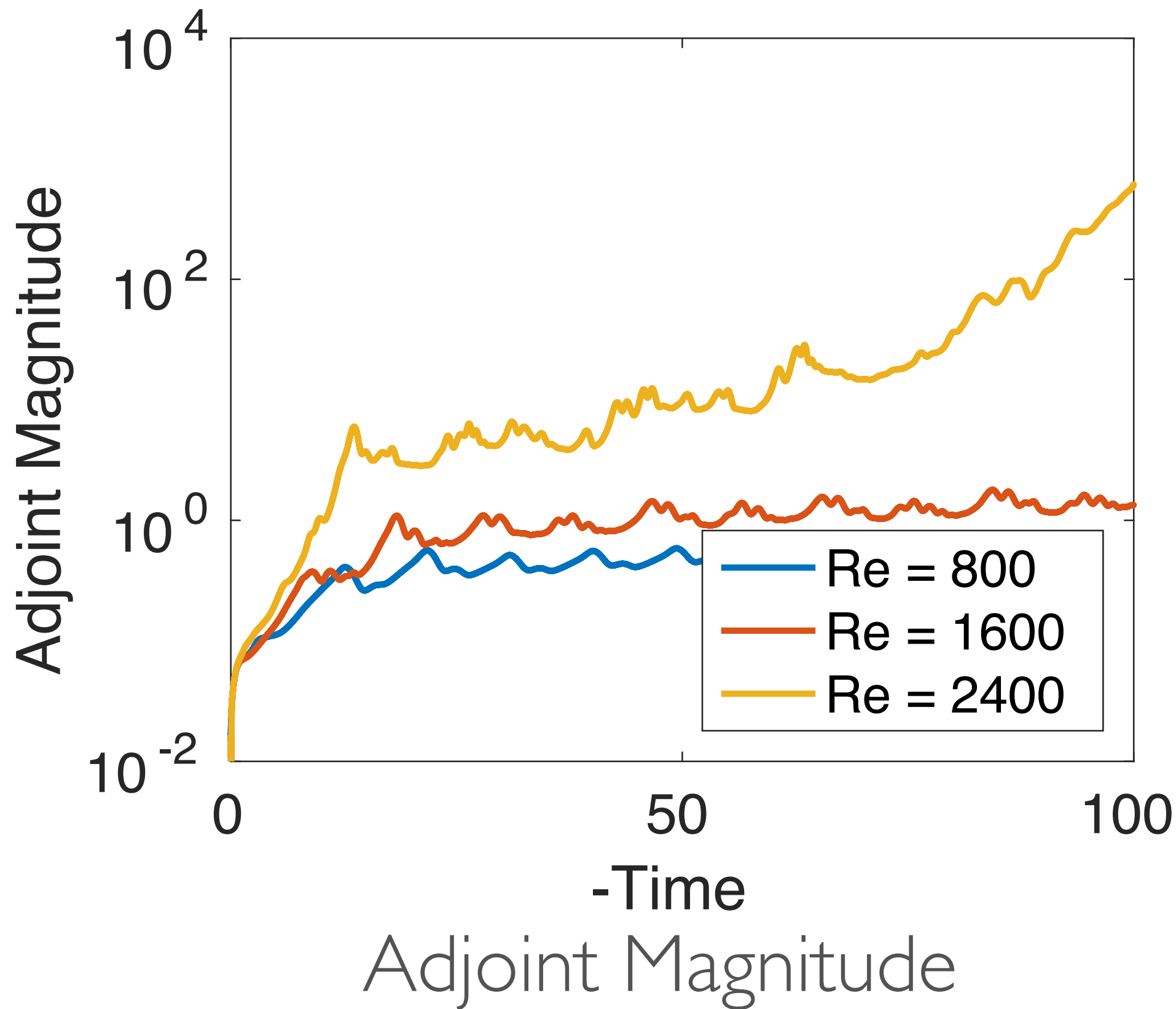
Directional Force Output



Adjoint Magnitude

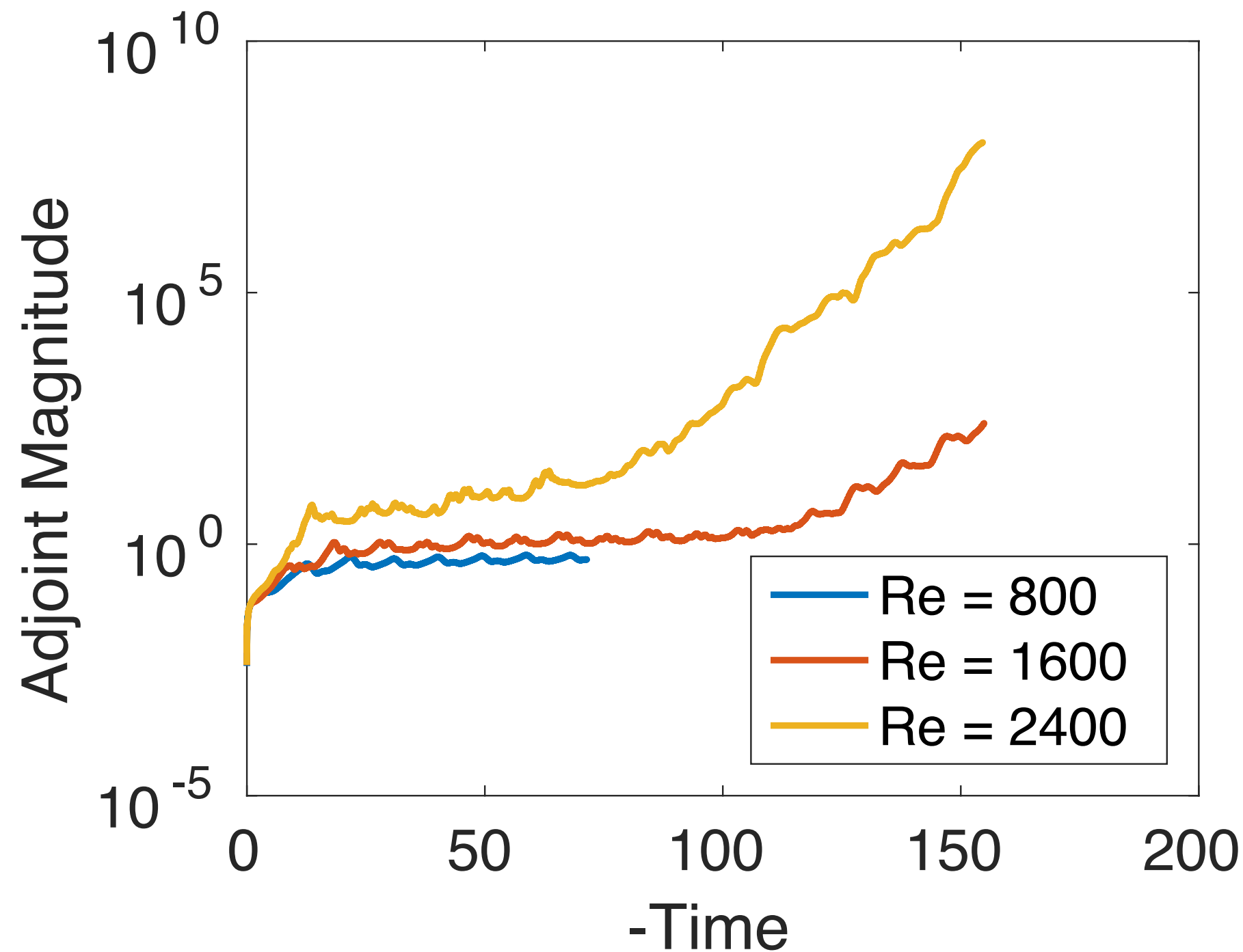
- With increasing Reynolds number simulated flow become chaotic
- Adjoint solution begins to grow unboundedly

# NACA0012, $Re = 800-2400$ , $\alpha = 10$



- With increasing Reynolds number simulated flow become chaotic
- Adjoint solution begins to grow unboundedly

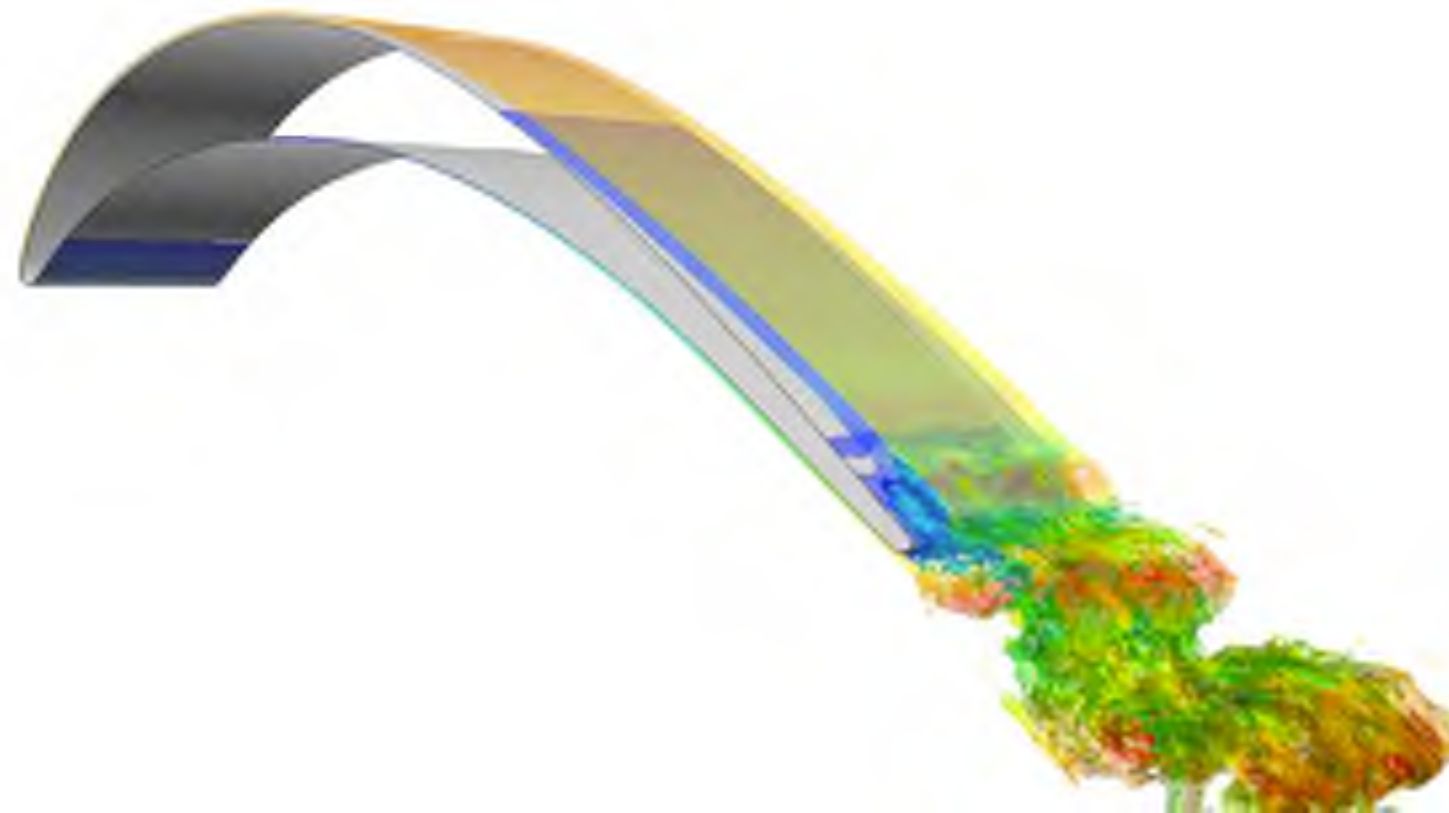
# NACA0012, $Re = 800-2400$ , $\alpha = 10$



Adjoint Magnitude

- Solution is in fact chaotic at  $Re = 1600$ , but growth rate is much slower than at  $Re = 2400$
- Windowing approaches may be successful at  $Re = 800, 1600$

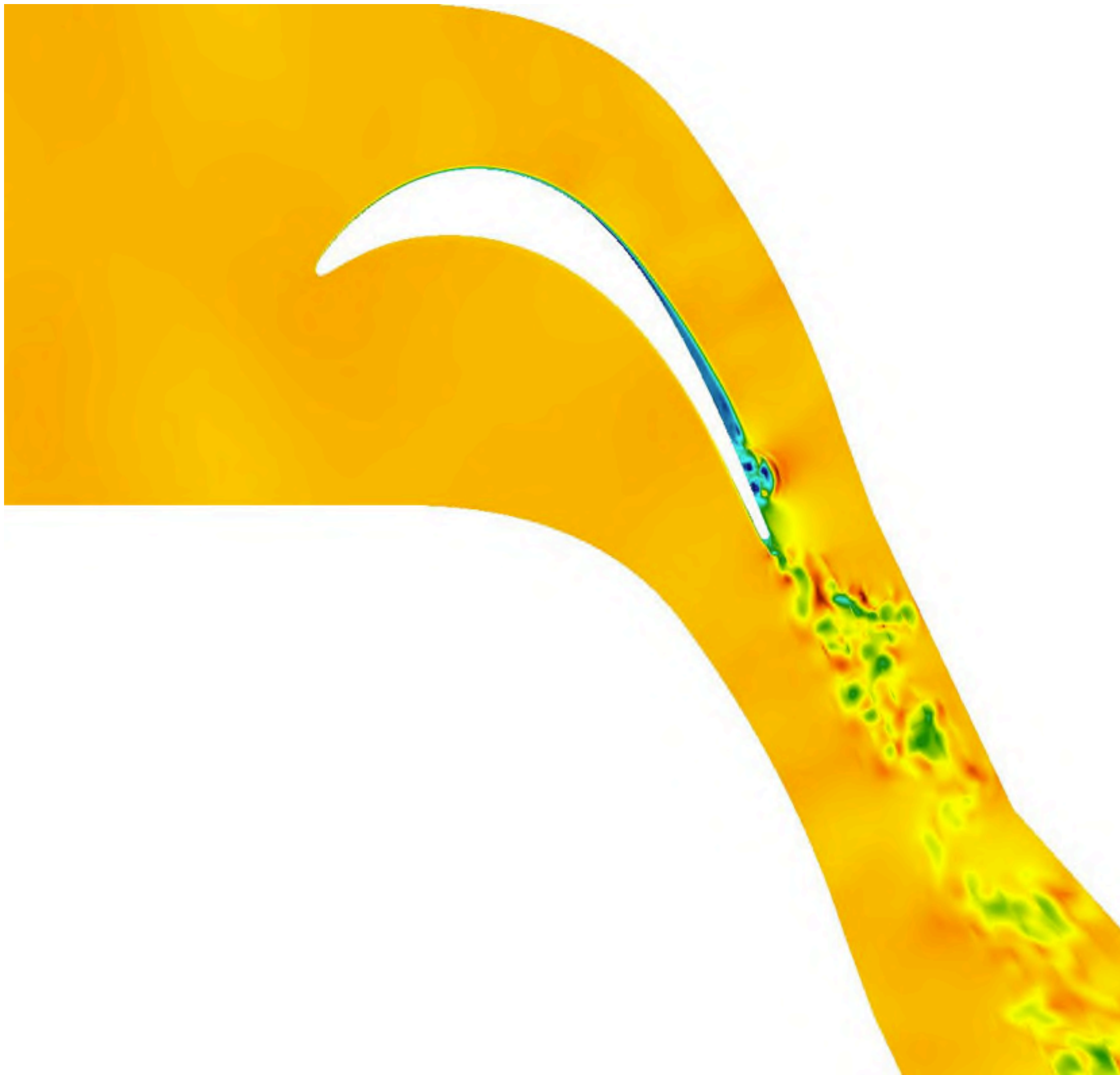
# T106c Low Pressure Turbine



- $Re = 80,000$ ,  $M_{inflow} = 0.243$ ,  $\alpha = 32.7$ ,  $M_{exit} = 0.65$
- Periodic BCs in span-wise and pitch-wise directions
- No free-stream turbulence
- Spanwise domain is 20% of chord



# Primal Solution



- Nearly steady flow upstream and over first 2/3 of blade
- Separation leading to transition/vortex shedding on suction-side of blade
- Fully turbulent wake

# Sensitivity to Inflow Boundary Condition

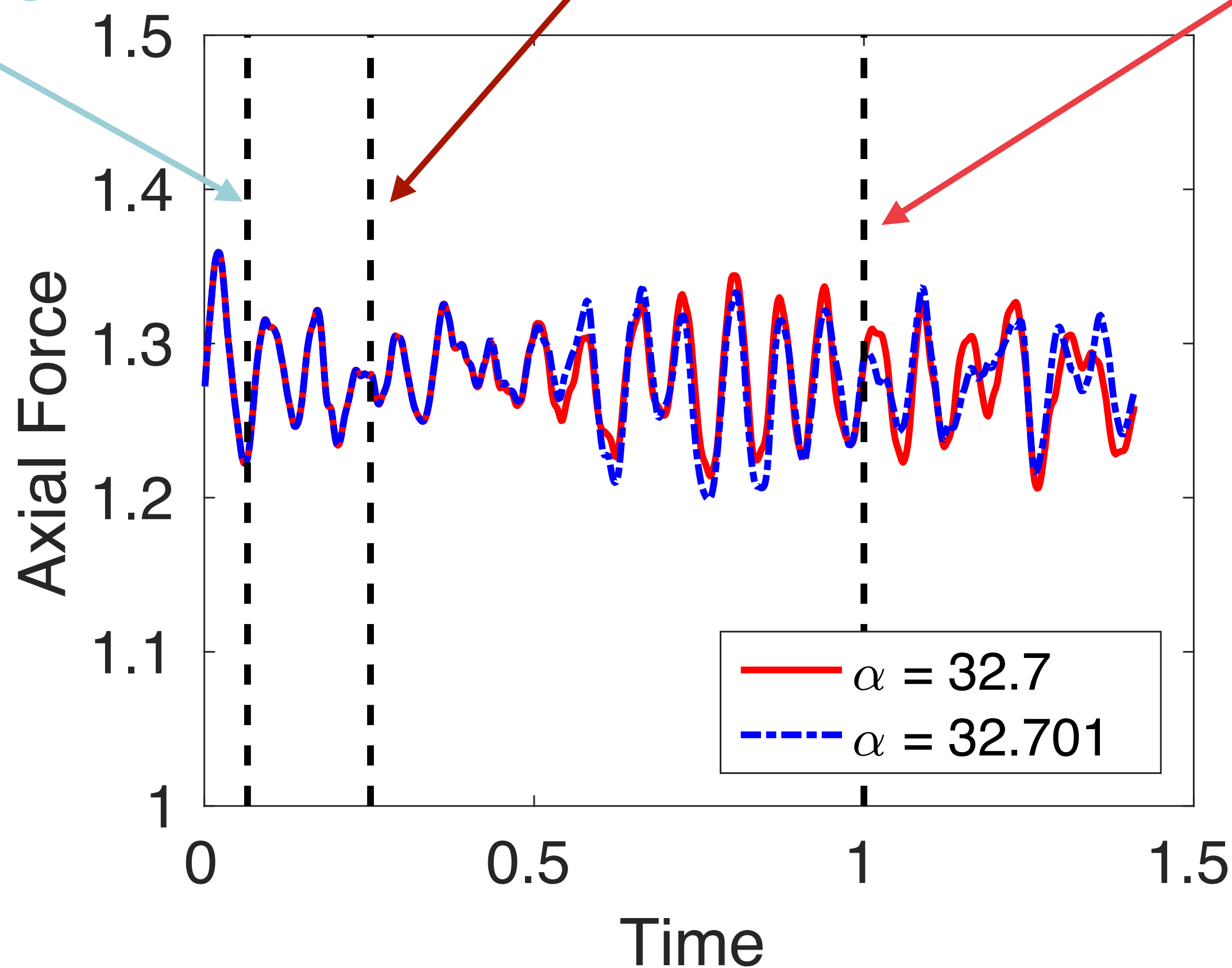


- Modify inlet flow angle from  $\alpha = 32.7$  to  $\alpha = 32.701$

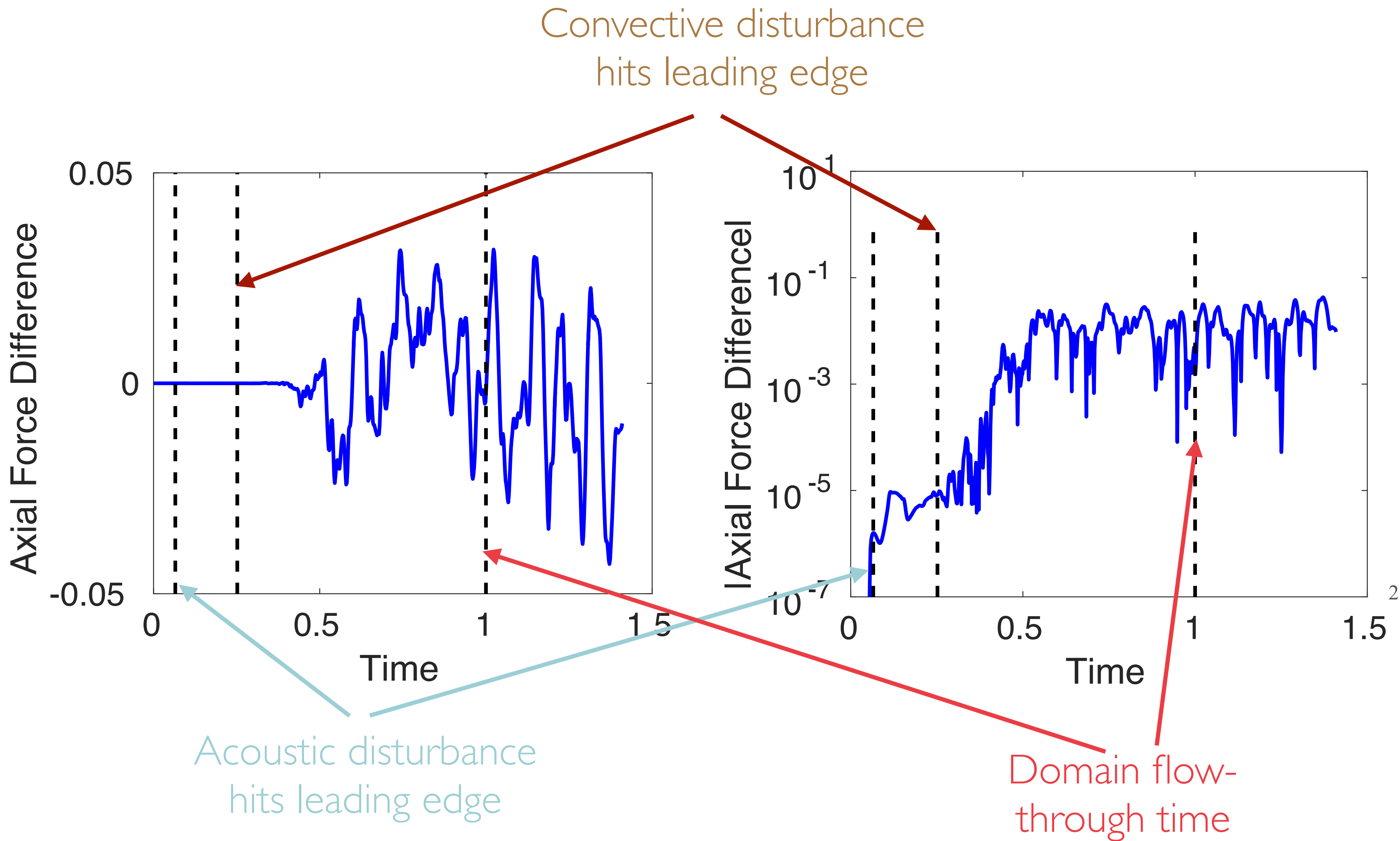
Acoustic disturbance  
hits leading edge

Convective disturbance  
hits leading edge

Domain flow-  
through time



# Sensitivity to Inflow Boundary Condition



# Adjoint of mean Axial Force

- Output is integrated axial force

$$\bar{J} = \frac{1}{T} \int_0^T F_x(u(\tau)) d\tau$$

- Also define output without temporal normalization

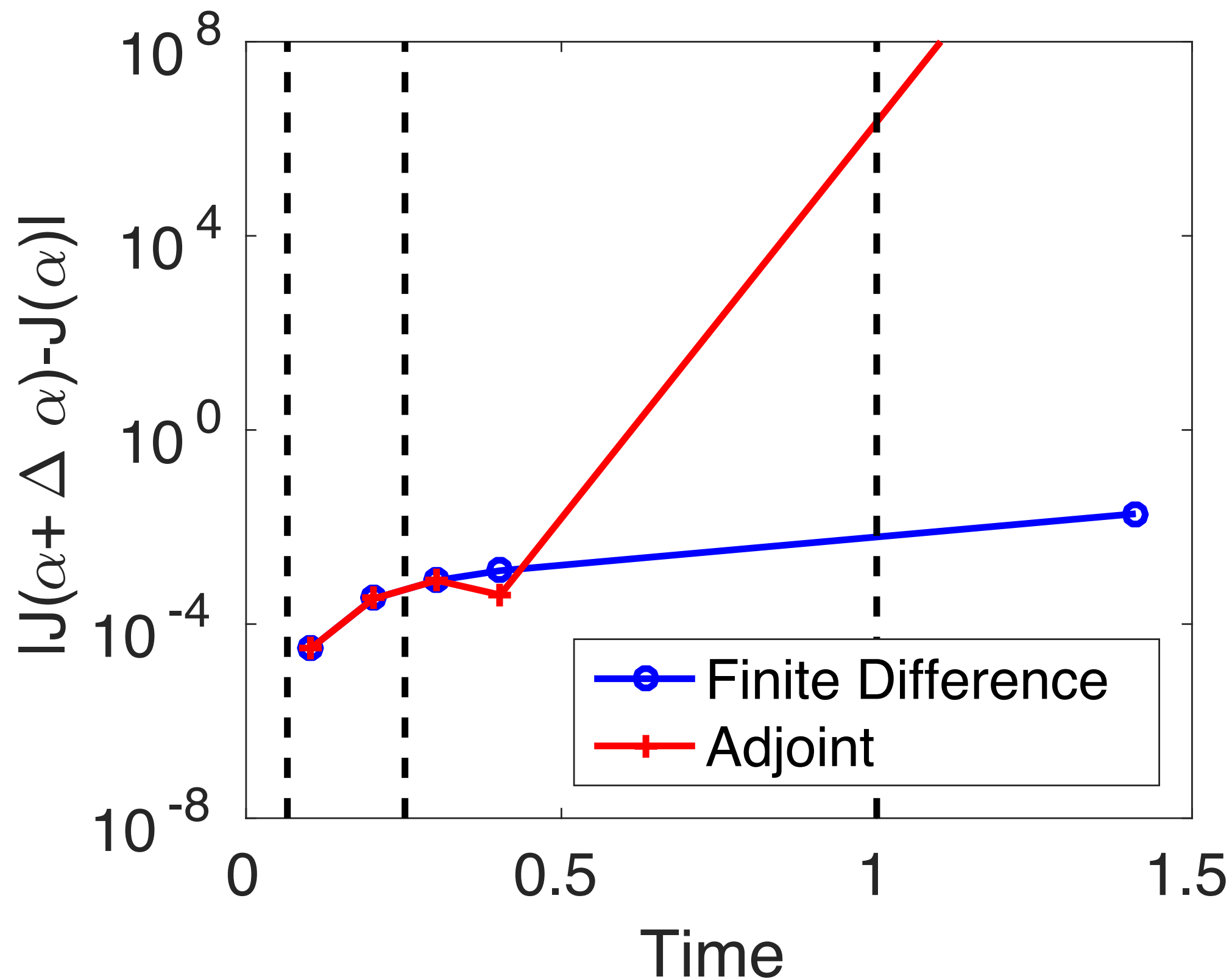
$$J(t) = \int_0^t F_x(u(\tau)) d\tau$$

Range:  $[-1 \text{ e}6, 1 \text{ e}6]$

# Sensitivity computed using adjoint

$$\Delta J(t) = J(t; \alpha + \Delta\alpha) - J(t; \alpha) = \int_0^t F_x(u(\tau; \alpha + \Delta\alpha)) - F_x(u(\tau; \alpha)) d\tau$$

$$\approx \int_0^t \Psi(\tau; t, \alpha)^T R(u(\tau); \alpha + \Delta\alpha)$$

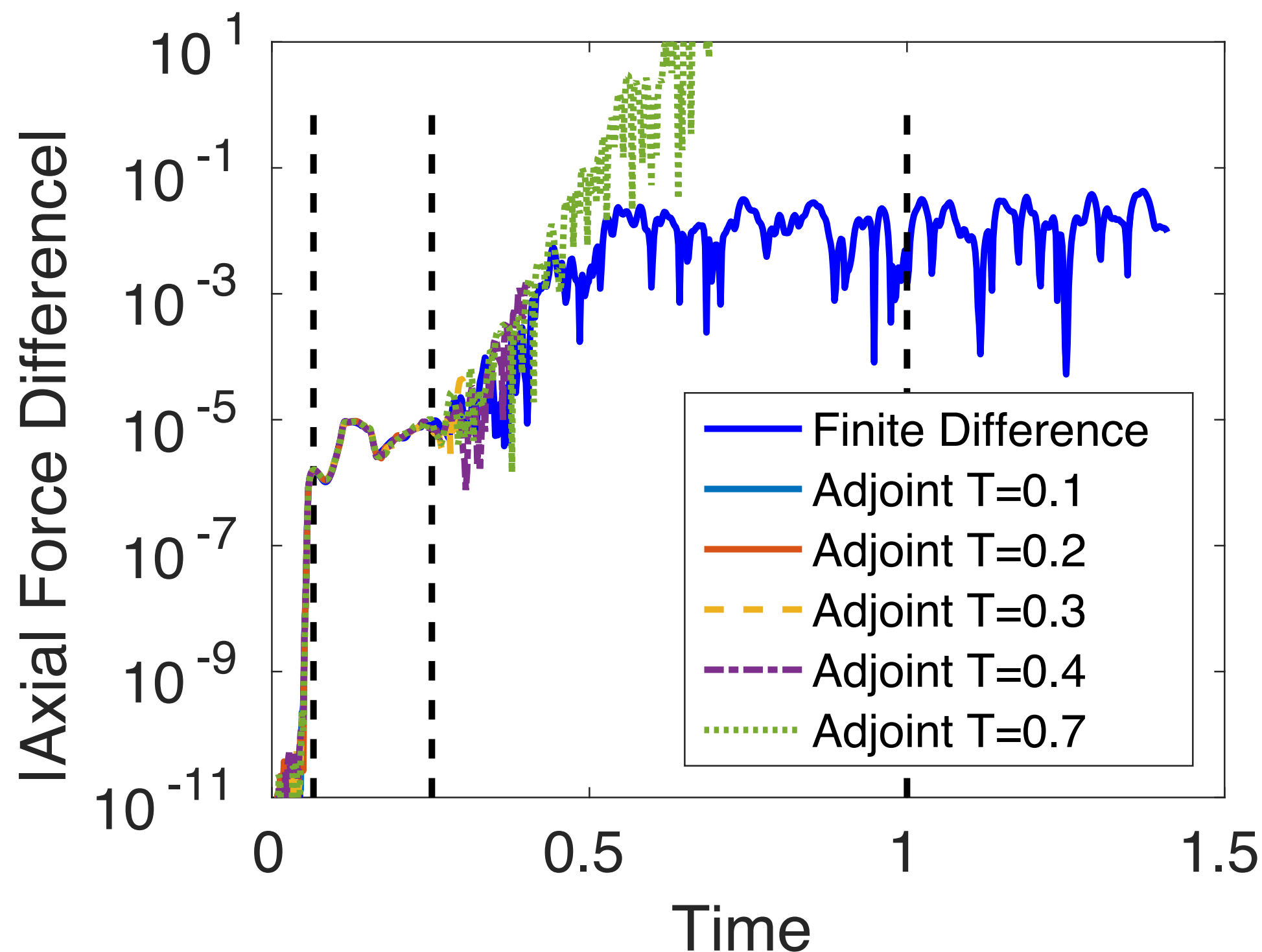




# Sensitivity computed using adjoint

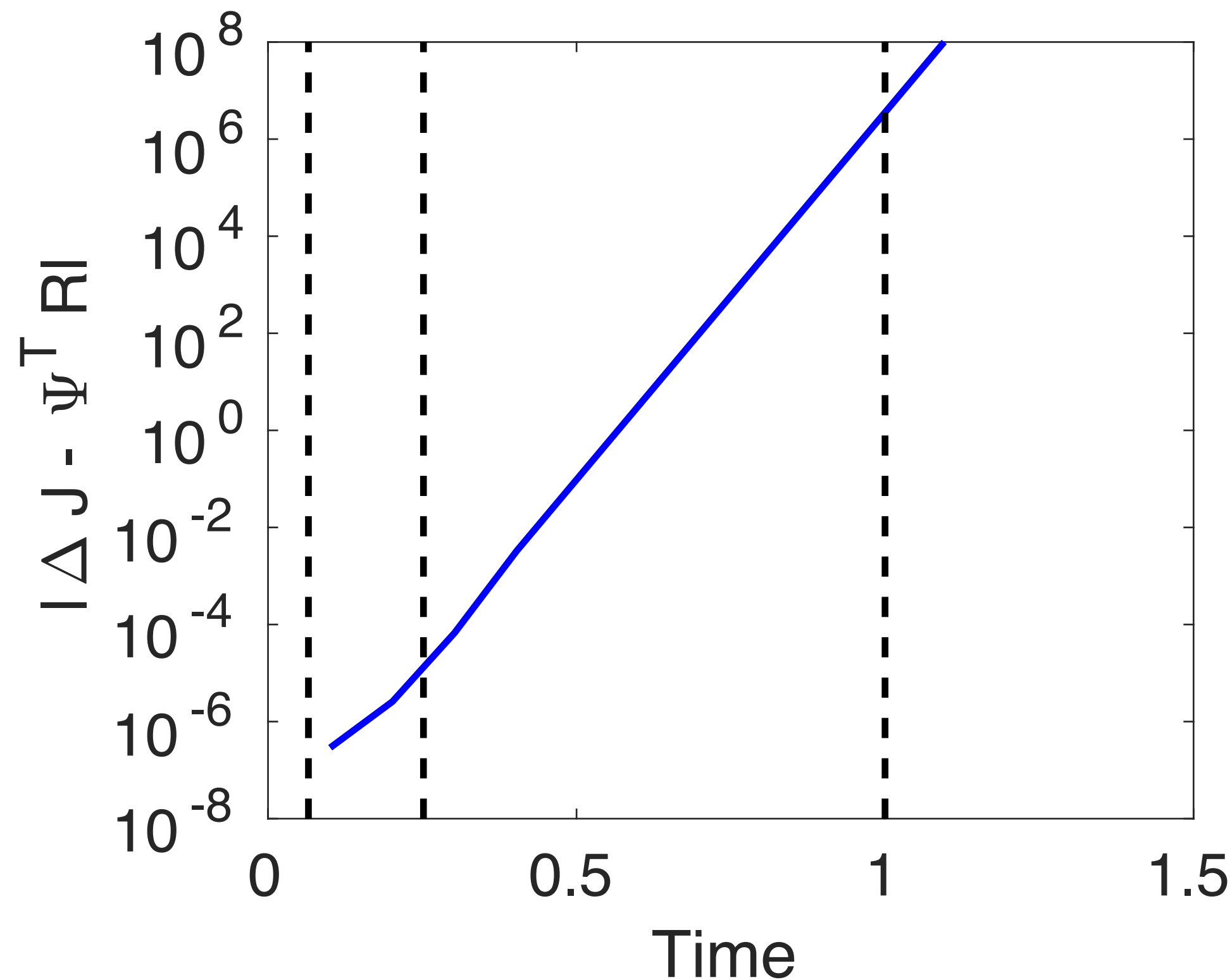
$$\Delta F_x(\tau) = F_x(u(\tau; \alpha + \Delta\alpha)) - F_x(u(\tau; \alpha))$$

$$?? \approx \Psi(t - \tau; t, \alpha)^T R(u; \alpha + \Delta\alpha)$$




- Approximation holds since flow upstream of blade is essentially time-independent
- Adjoint correctly captures sensitivity in part of flow upstream of separation

# Sensitivity computed using adjoint



- Sensitivity computed using adjoint only valid for very short time windows
- Adjoint computed using long time window blows up
- Sensitivity computed using short time window, not representative long time behaviour

# Graphical demonstration of concepts

- 
- Adjoint correctly captures sensitivity in part of flow upstream of separation
  - Sensitivity computed using adjoint only valid for very short time windows
  - Sensitivity computed using short time window, not representative long time behaviour

# Adjoint-based Error Estimation

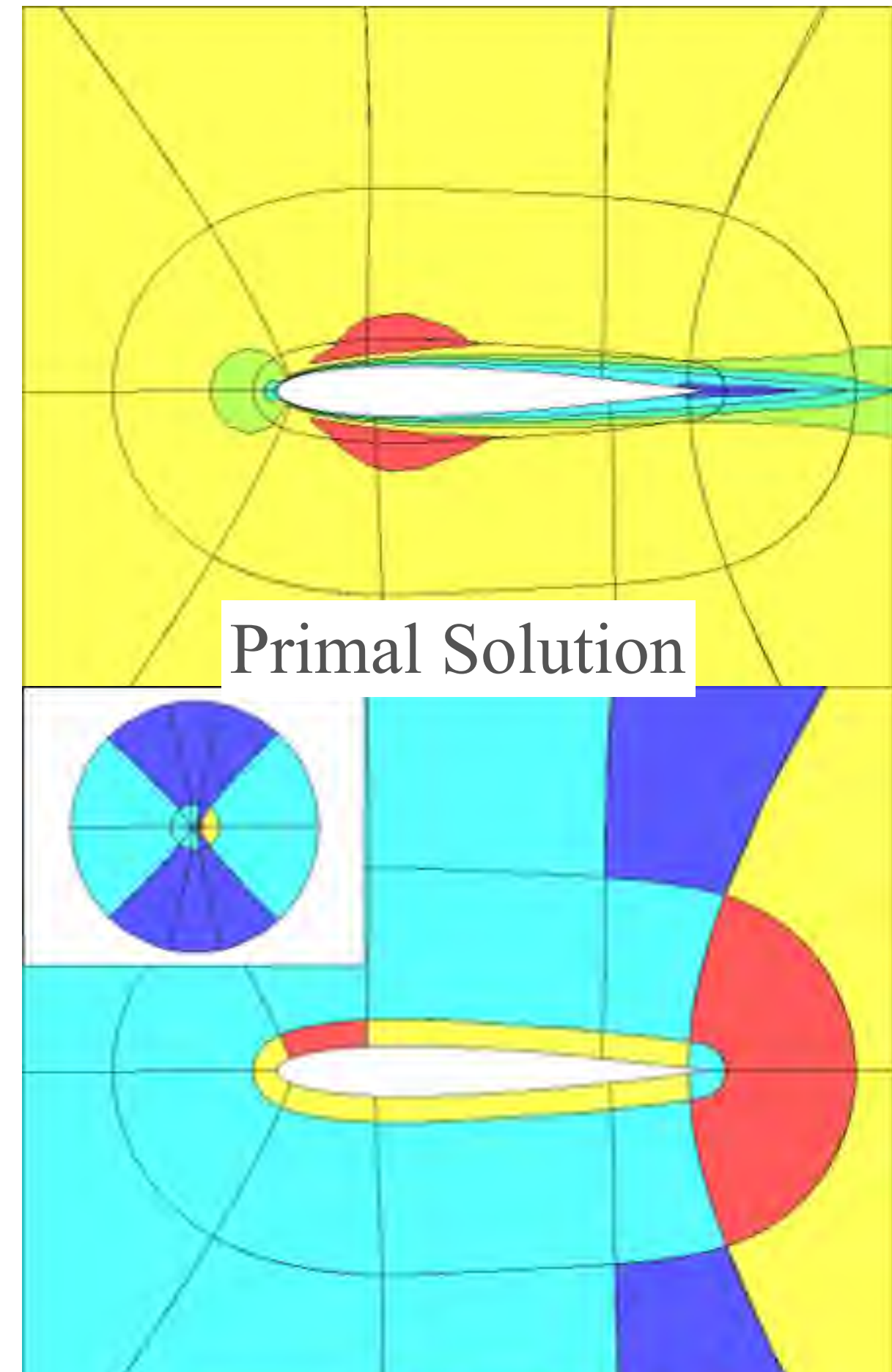
- Estimate error using dual-weighted residual method (Becker & Rannacher 1995)

$$\epsilon = J(u) - J(u_H) \approx R_H(u_H, \psi_h)$$

- Localize error

$$\epsilon_\kappa \equiv R_H(u_H, \psi_h|_\kappa)$$

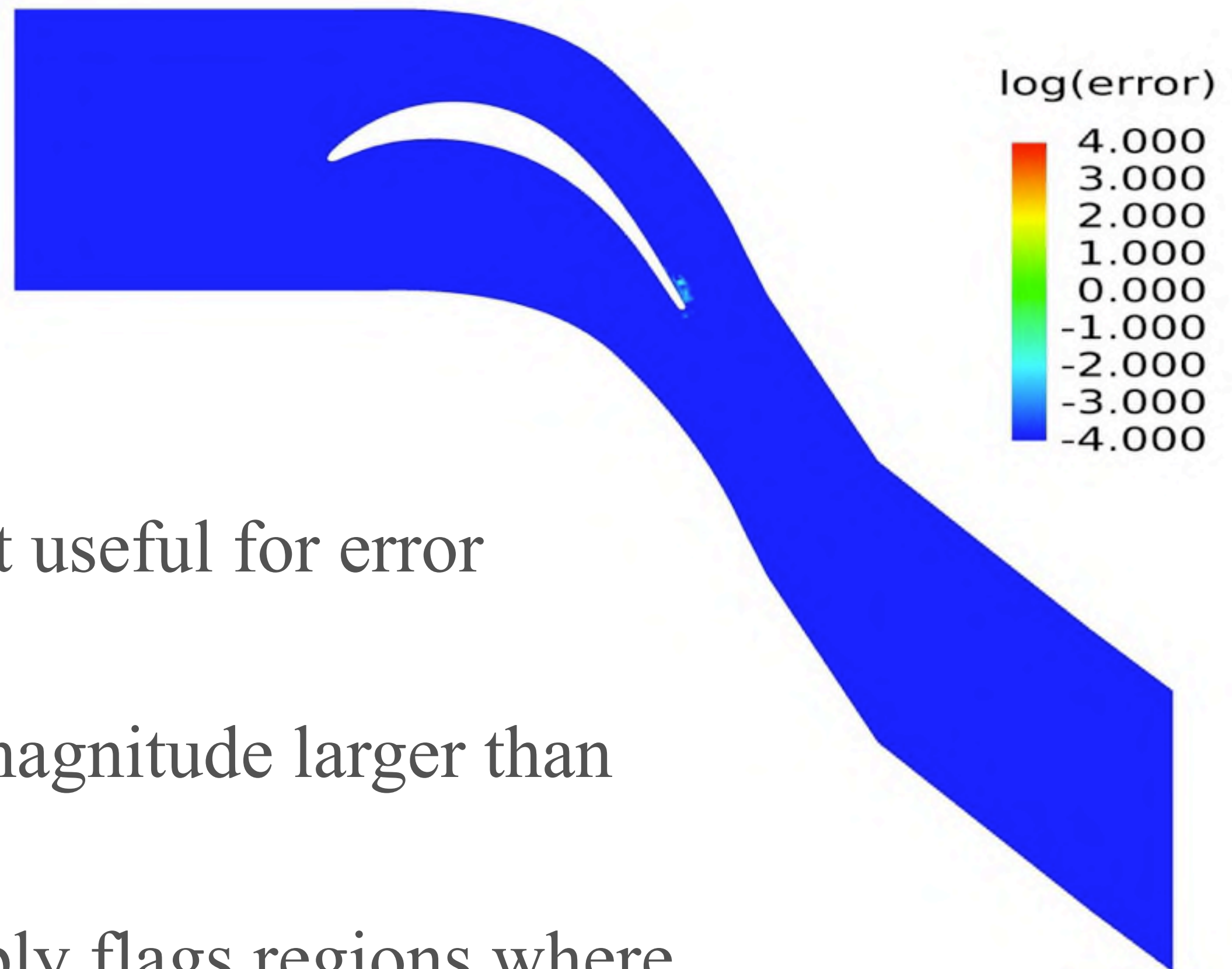
- Flag elements with largest error for refinement



Element-based error-indicator



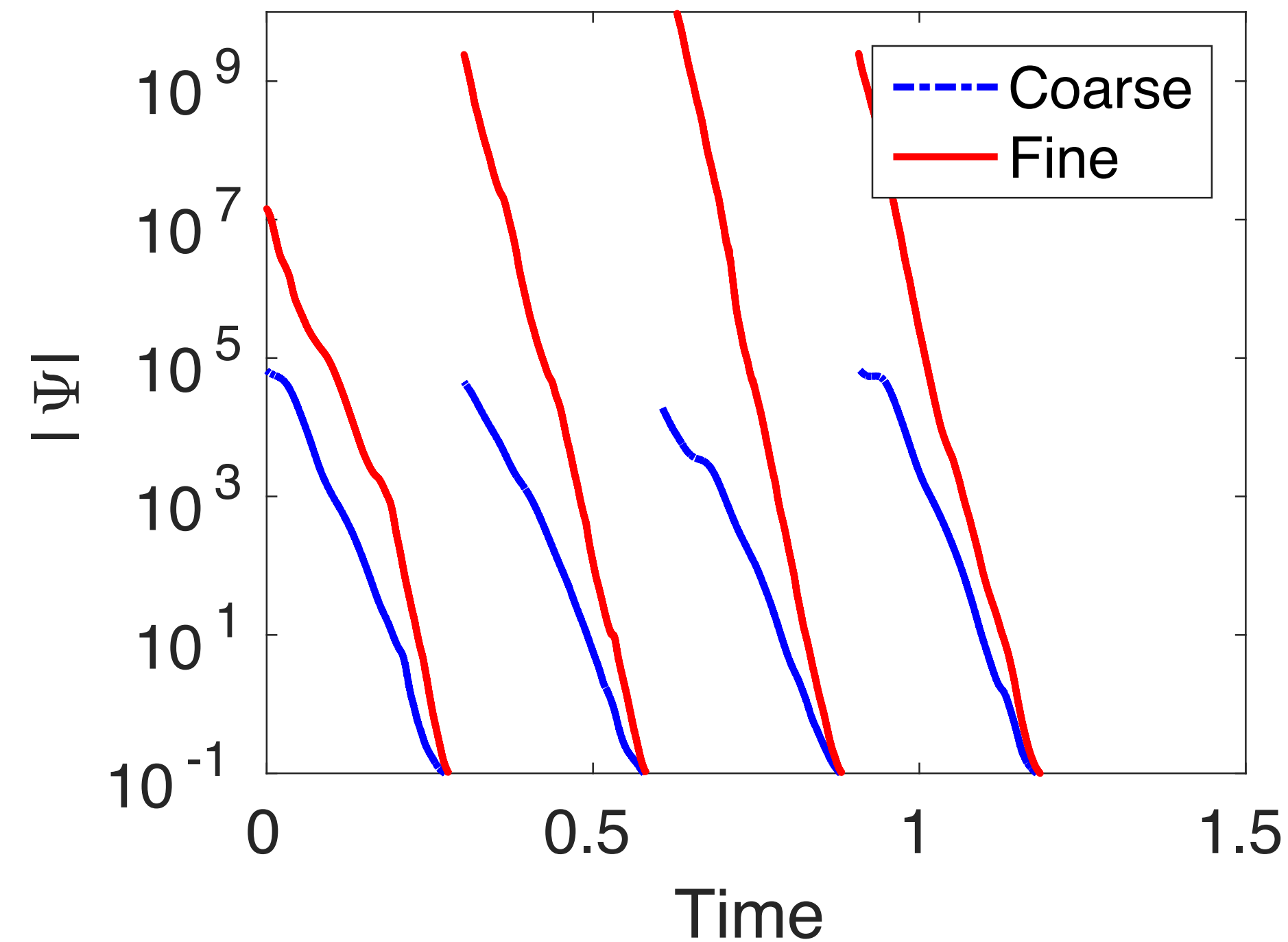
# Adjoint-based error indicator



- Unbounded adjoint not useful for error estimation
- Estimate is orders of magnitude larger than actual signal
- Error localization simply flags regions where adjoint is large



# Adjoint growth with mesh resolution



- Refined mesh has essentially double mesh resolution near separation region
- Increase mesh resolution results in faster growth of adjoint (i.e. larger Lyapunov exponent)
- Adaptation mechanism is not convergent

# Summary



- Presented space-time adjoint solver for turbulent compressible flows
- Confirmed failure of traditional sensitivity methods for chaotic flows
- Assessed rate of exponential growth of adjoint for practical 3D turbulent simulation
- Demonstrated failure of short-window sensitivity approximations.



# Questions??

## Outlook/Future Work:

- Lyapunov exponents, least-square shadowing and beyond...